

## ***RHESSI* Observations of the Solar Flare Iron-Line Feature at 6.7 keV**

K. J. H. Phillips

*National Research Council Senior Research Associate, NASA Goddard Space Flight Center,  
Greenbelt, MD 20771, U.S.A.*

kennethjhphillips@yahoo.com

C. Chifor

*Department of Applied Mathematics and Theoretical Physics, Centre for Mathematical  
Sciences, Wilberforce Road, Cambridge CB3 0WA, United Kingdom*

B. R. Dennis

*NASA Goddard Space Flight Center,  
Greenbelt, MD 20771, U.S.A.*

### **ABSTRACT**

Analysis of *RHESSI* 3–10 keV spectra during 30 solar flares is reported. This energy range includes thermal free–free and free–bound continuum and two line features, at  $\sim 6.7$  keV and  $\sim 8$  keV, principally due to highly ionized iron (Fe) ions. We used the continuum and the flux in the so-called Fe-line feature at  $\sim 6.7$  keV to derive the electron temperature  $T_e$ , the emission measure, and the Fe-line equivalent width as functions of time in each flare. The Fe/H abundance ratio in the flares is derived from the Fe-line equivalent width as a function of  $T_e$ . To minimize instrumental problems with high count rates and effects associated with multi-temperature and nonthermal spectral components, spectra are presented mostly during the flare decay phase, when the emission measure and temperature were smoothly varying. We found flare Fe/H abundance ratios that are consistent with the coronal abundance of Fe (i.e. 4 times the photospheric abundance) to within 20% for at least 17 of the 30 flares; for 7 flares, the Fe/H abundance ratio is possibly higher by up to a factor of 2. We find evidence that the Fe XXV ion fractions are less than the theoretically predicted values, by up to 60% at  $T_e = 12$  MK; the observed  $N(\text{FeXXV})/N(\text{Fe})$  values appear to be displaced from the most recent theoretical values by between 1 and 3 MK.

*Subject headings:* Sun: X-rays, gamma rays—Sun: flares

Printed on October 3, 2005

## 1. Introduction

The *Reuven Ramaty High Energy Solar Spectroscopic Imager* (*RHESSI*) was launched on 2002 February 5 and has since been returning high-quality X-ray and gamma-ray images and spectra of solar flares at energies between  $\sim 3$  keV and 17 MeV (Dennis et al. 2004). Here we present an analysis of *RHESSI* observations of thermal spectra in the 4–10 keV range for 30 flares. This energy range includes thermal free–free and free–bound continuum and two line features, one at  $\sim 6.7$  keV referred to as the Fe-line feature and the other at  $\sim 8$  keV referred to as the Fe/Ni-line feature. They are both due principally to highly ionized (mostly He-like and Li-like) iron (Fe) ions with the higher energy feature including some lines from highly ionized nickel. Both these line features are clearly visible in *RHESSI* flare spectra once the plasma temperature is above  $\sim 20$  MK. The spectral resolution of the *RHESSI* detectors –  $\sim 1$  keV FWHM – is inferior to that of crystal spectrometers (e.g. the Bent Crystal Spectrometer BCS on *Yohkoh*) in this energy range. Such spectrometers typically have an energy resolution of a few eV, enough to resolve individual lines in the 6.7 keV feature. However, most crystal spectrometers operating in this range cannot measure the continuum very accurately since it is overwhelmed by a fluorescence background. Also, because of their limited spectral coverage, they have generally not been used to detect the Fe/Ni line feature, apart from an early observation of Neupert et al. (1969). *RHESSI* covers a much broader energy range and is able to measure both line features and the continuum emission.

Measurements with *RHESSI* of the ratios of the total emission in the Fe-line feature to the nearby continuum, or more specifically the equivalent width, are therefore possible. If nonthermal contributions to the continuum are negligible and if the continuum is emitted by an isothermal plasma with electron temperature  $T_e$  and emission measure  $\int_V N_e^2 dV$  ( $V$  is the emitting volume and  $N_e$  the electron density), the slope of the logarithm of the continuum flux with energy  $E$  gives  $T_e$ , and the continuum flux gives the emission measure. For the 30 flares analyzed here, the observed equivalent widths of the Fe-line feature as a function of  $T_e$  were compared with the theoretical dependence of the equivalent width on  $T_e$  – the latter is well known from ion fractions, line excitation rates, and an assumed value for the Fe abundance (Phillips 2004). The Fe abundance in flare plasmas can thus, in principle, be determined as a function of time for each flare. We often found small differences between the temperature dependence of the theoretical and observed equivalent widths, which may

be attributable to incorrect theoretical Fe ion fractional abundances. This shows a need for the revision of ionization or recombination rate coefficients for highly ionized Fe ions.

Preliminary results have already been given for a similar analysis of one flare by Dennis et al. (2005). The flux ratio of the Fe-line feature to the Fe/Ni line feature is a function of  $T_e$  alone, independent of the iron abundance, and *RHESSI* measurements of this ratio during flares are the subject of a separate paper by Caspi et al. (2005).

## 2. *RHESSI* Instrumental Effects

Instrumental details of *RHESSI* are given by Lin et al. (2002), Smith et al. (2002), and Hurford et al. (2002). The *RHESSI* spectrometer consists of an array of nine cooled and segmented germanium detectors. X-ray imaging and spectroscopy up to several hundred keV is carried out using the 1-cm-thick front segments with the rear segments operated in anti-coincidence to reduce the background. Imaging is achieved through the use of rotating modulation collimators located in front of the detectors, resulting in a time-modulated signal that can be analyzed to give spatial information. For 4–10 keV X-rays, the energy resolution (FWHM) depends on the detector, ranging from  $\sim 1$  keV for detectors 3 and 4,  $\sim 1.5$  keV for detector 5, and  $> 3$  keV for detector 2. The lower-energy threshold for all detectors is set at 3 keV except for detectors 2 and 7 for which it was generally  $\gtrsim 10$  keV during the times of the observations we analyzed. The spectral output from individual detectors (detector 4 for most of the work reported here) or the summed output of a combination of detectors (excluding detectors 2 and 7) may be analyzed independently.

Each detector views the flare emission through a beryllium cryostat window and aluminized-mylar thermal blankets. At high photon count rates encountered during flares, attenuators mounted on frames in front of the detectors move into place to mitigate pulse pile-up and detector saturation problems that result from the huge ( $> 10^5$ ) dynamic range in flare intensities detectable with *RHESSI*. The attenuators consist of two sets of thin aluminum disks with one set thicker than the other. Each disk has the same diameter as a detector front segment (6.15 cm) to attenuate the solar photon flux that reaches the detector, but has a thinner circular region in the center to allow some low-energy transmission. Under normal circumstances, both sets of attenuators are held out of the detector lines of sight to the Sun. This is referred to as the A0 attenuator state. As the X-ray counting rate from a flare increases above a prescribed level, the ‘thin’ attenuators are automatically inserted into the fields of view. This is called the A1 state. If the emission rises still further to another prescribed count rate level, then the ‘thick’ attenuators are also inserted. This is called the A3 state. (The ‘thick attenuator only’ or A2 state is not used as it provides very similar

attenuation to the A3 state.) Insertion of the thin and thick attenuators results in a reduction in count rate, particularly at low energies, since the transmission drops very steeply as a function of decreasing energy. The transmission fraction drops to 1% at  $\sim 4$  keV in the A0 state,  $\sim 8.5$  keV in the A1 state, and  $\sim 13$  keV in the A3 state. Estimates of the energy-dependent attenuation of the thin and thick attenuators are available from pre-launch measurements (Smith et al. 2002), and are incorporated in the *RHESSI* analysis software package.

The lowest energy photon flux that can be reliably determined in the different attenuator states depends not only on this increasing attenuation at the lower energies but also on the K-escape phenomenon. An incident photon with an energy above the germanium K-edge at 11.1 keV can ionize a germanium atom by ejecting one of its two K-shell electrons. There is a certain probability that the ionized atom will, almost instantaneously, emit a  $K\alpha$  photon at  $\sim 9.25$  keV or a  $K\beta$  photon at  $\sim 10.3$  keV. These photons, in turn, may be absorbed in the detector front segment, thus giving a signal proportional to the full energy of the incident photon. Alternatively, it may escape from the detector so that the resulting signal is smaller than that expected for the given incident photon energy. These K-escape events appear in the count-rate spectrum at an energy equal to the incident photon energy minus the energy of the escaping K-line photon. Since, in the A1 and A3 attenuator states, the attenuation at these low energies is very high, there are very few “true” counts recorded from incident photons with those energies. In fact, the number of K-escape events exceeds the number of “true” events at energies below 5–6 keV and no information can be obtained about the incident photon spectrum at these energies. In practice, for reasons at present unknown, there are usually more counts below 5–6 keV than predicted from our rather accurate knowledge of the K-escape phenomenon. Consequently, we have limited our spectral fits to higher energies, i.e.  $> 5$  keV, where the predicted and observed count rates can be made to agree for reasonable model parameters as indicated by the  $\chi^2$  values.

At very high photon count rates, spectral distortion takes place because of “pulse pile-up.” This arises because the instrument electronics are unable to separate the electronic pulses produced by two photons arriving in a detector within a few  $\mu\text{s}$  of each other. The result is that the two photons are recorded as a single event with an energy that can be as high as the sum of the energies of the two photons. In practice, pulse pile-up begins to appear in the count rate spectrum as excess counts at an energy roughly twice the energy of the peak count rate, i.e. at  $\sim 14$  keV in the A0 state,  $\sim 20$  keV in A1, and  $\sim 35$  keV in the A3 state. The analysis software allows some correction for pulse pile-up but with considerably increased uncertainty in the estimated temperature and emission measure. This is especially significant at times of increasing count rates to a level immediately before the attenuators are inserted and times of decreasing count rates to a level immediately after the attenuators

are removed.

Another rate-dependent effect is a change in the energy calibration such that the apparent energy of the Fe line at  $\sim 6.7$  keV increases by up to 0.3 keV as the rate increases. This is probably a fixed increase in the electronics baseline so that the increase is independent of energy. Thus, it is only significant at the lower energies. Nevertheless, it prevents us, at present, from exploiting the temperature diagnostic offered by the slight increase in the Fe-line centroid energy with  $T_e$  ( $\sim 0.1$  keV over  $T_e = 10 - 30$  MK: Phillips (2004)). This effect is further complicated by the fact that the detector count rates are rapidly modulated by the collimators as the spacecraft rotates. Thus, in addition to the energy calibration changing at high rates, the effective energy resolution is degraded as well.

With the seven detectors usable for soft X-ray spectral analysis, we are able to check the measured sensitivities of each detector by comparing the derived photon spectra in each case for particular time intervals. In Fig. 1, we show the comparison of the derived photon spectra for a time interval when *RHESSI* was in the A1 state. Although the photon fluxes determined from the seven detectors independently agreed to better than  $\sim 20\%$  at the higher end of the energy range chosen for analysis ( $\sim 20$  keV), the agreement at lower energies is less satisfactory. There was typically a factor 2.5 spread from the minimum to maximum derived photon fluxes at  $\sim 5$  keV. This disagreement may be connected with increased uncertainties in the attenuation at low energies, which is a very steep function of energy, and with the origin of the excess counts over and above the K-escape events. Most of the results in the remainder of this work are from spectra observed with detector 4, which has relatively good spectral resolution ( $\sim 1$  keV FWHM) and, in Fig. 1, produces a photon spectrum close to the mean of all spectra.

Analysis of *RHESSI* spectra requires the reliable determination of background emission (Smith et al. 2002). All but three of the thirty flares chosen for analysis here had peak *GOES* emission exceeding M1, so near maximum the flare soft X-ray count rates were at least a factor of 100 higher than the background rates at all the energies used in our fits, i.e.  $\lesssim 20$  keV. However, spectra during periods late in each flare required taking the background spectrum into careful consideration. The background counts are due predominantly to cosmic ray and trapped particle radiation, and the rate varies over the spacecraft orbit, being generally higher at higher north and south geomagnetic latitudes. The background energy spectrum is made up of a continuum and several lines, the most relevant of which for our purposes being the strong Ge K-line feature at  $\sim 10.5$  keV due to the activation of the germanium detectors.

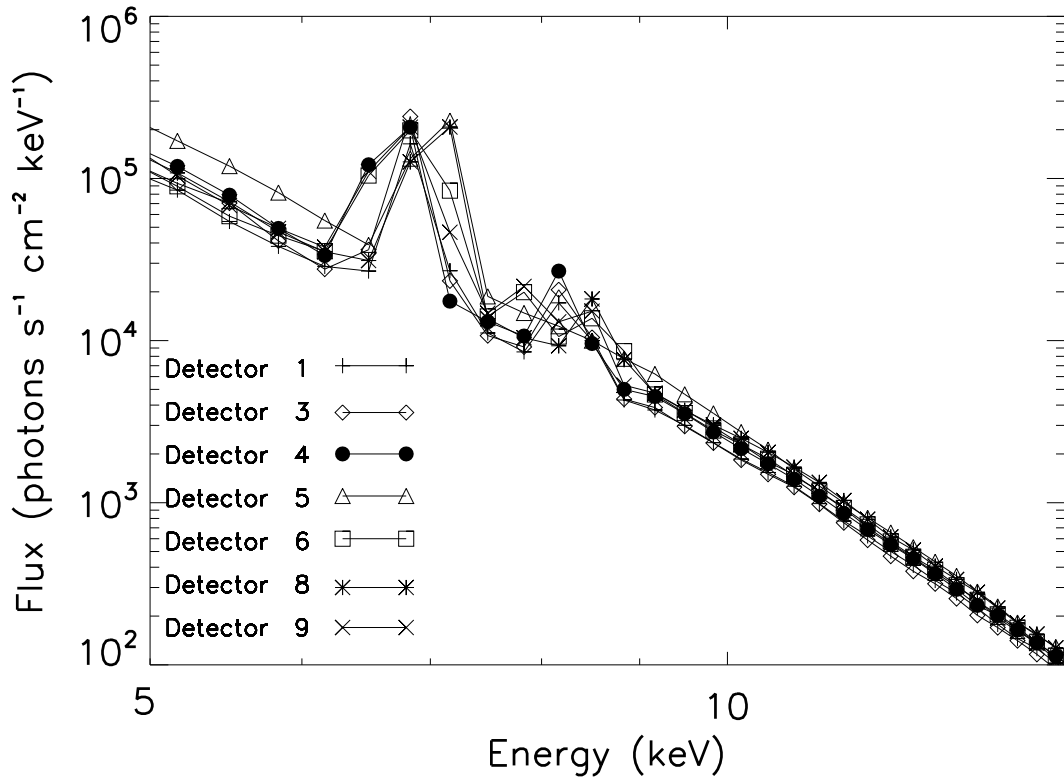


Fig. 1.— Photon spectra obtained from analysis of output from *RHESSI* detectors 1, 3, 4, 5, 6, 8 and 9 over a 20-s interval at 10:01 U.T., during the decay of the flare of 2003 August 19.

### 3. Data Analysis

The *RHESSI* data analysis software available in the Solar Software tree (SSW) requires that the spectral analysis be done in two stages. In the first stage, the *RHESSI* data files containing the raw time-ordered data covering the times of interest are read in and count rate spectra (counts  $\text{s}^{-1}$  per detector) are extracted over user-supplied time intervals, energy ranges, and energy bins. For most of the flares analyzed here, detector 4 spectra were extracted, and the energy bins chosen were 1/3 keV wide from 3 to 20 keV, and 1 keV wide from 20 to 100 keV. Corrections are made by the software for detector live time, decimation, and energy calibration. Optionally, pulse pile-up corrections can be made. These are significant if the count rate exceeds  $\sim 1000$  counts  $\text{s}^{-1}$ , and were applied consistently in our analysis. The output from this first stage of the analysis consists of two computer files, one containing the count rate spectra for the time intervals chosen by the user, the other containing the spectrometer response matrix (srm) including the off-diagonal matrix elements.

In the second analysis stage, the two output files from the first-stage are read by an object-oriented program known as the Object Spectral Executive (OSPEX). At this stage, the background is subtracted and instrument-independent photon spectra are derived from the measured count-rate spectrum.

Background subtraction is relatively simple for weaker flares where the attenuators remain in the A0 state, but becomes more complicated when the attenuator state changes during the flare of interest. For flares in the A0 state, short intervals before and/or after the flare were used to obtain a background spectrum. Linear or low-order polynomial interpolation between these background intervals can give a reliable prediction of the background during the flare as long as periods of particularly high background levels are avoided. The selection of the background spectrum to subtract is usually more difficult in the A1 and A3 attenuator states, however. This is because there is usually no time period available either before or after the flare in the same attenuator state that can be used to give the background spectrum *in that state*. This is because there is often low-level X-ray emission from somewhere on the Sun both before and after the flare of interest that is detected in the A0 state but gives a much lower count rate in the A1 or A3 states. In such cases, we used the simplest approach of taking the spectrum measured during the nighttime part of the orbit since then there can be no solar emission enhancing the background. These background concerns are only important for times when the estimated background count rates at any given energy are greater than about 10% of the measured count rate from the flare.

With the background spectrum subtracted, the program proceeds iteratively to find the parameters of a user-selectable model photon spectrum (see below) that best fits the data

for each time interval. After deciding on the components of the model photon spectrum and reasonable starting parameters, the program uses the spectral response matrix to calculate the count rate spectrum that would be produced by the model photon spectrum. This calculated spectrum is then compared with the measured background-subtracted count rate spectrum and a  $\chi^2$  value is obtained. The model parameters are adjusted and the process repeated until a minimum value of  $\chi^2$  is obtained. If the value of the reduced  $\chi^2$  ( $\chi^2$  divided by the number of degrees of freedom) is acceptable ( $\lesssim 1$ ), then the best-fit parameters can be considered to be reliable for the particular assumed model photon spectrum.

The assumed model photon spectrum we used included the thermal free-free and free-bound continuum, a multiple power-law function for the nonthermal component (when needed), and up to three lines with Gaussian profiles for the Fe-line feature, the Fe/Ni line feature, and a residual instrumental line at  $\sim 10.5$  keV. In the version of OSPEX that we used, the model thermal photon spectra are from the MEKAL (Mewe et al. 1985) spectral code with cosmic element abundances. We fitted the observed count rate spectra by taking the continuum function of the MEKAL code with first-guess values for  $T_e$  (to define the energy dependence of the continuum) and emission measure (to define the flux at a particular energy) and with Gaussian line features at energies of  $\sim 6.7$  keV and  $\sim 8.0$  keV with first-guess total fluxes to approximate the Fe-line and Fe/Ni line features. These line energies are approximately the theoretical values for  $T_e \sim 20$  MK. We allowed the energies of these line features to “float” as free parameters, but only over a  $\pm 0.2$  keV range as the lines are unlikely to be displaced by more than this, either by energy calibration changes or actual changes due to the different intensities of lines making up the features at different temperatures. The line widths were generally taken to be 0.1 keV (FWHM) to match the energy range of the groups of lines forming each feature; the exact widths are usually irrelevant as they are much less than the spectral FWHM resolution of  $\sim 1$  keV for detector 4. However, at very high count rates, the line widths were allowed to float also to allow for the slight degradation of spectral resolution. The goodness of fit measured by the reduced  $\chi^2$  requires estimated uncertainties, both statistical (i.e. in the count rates) and systematic. The default value for the systematic uncertainties of 5% in the software was used in this analysis; decreasing this value has little effect on the best-fit spectral parameters, in general.

For most of the 30 flares analyzed, we examined spectra over a time range which generally included the rise phase, the flare maximum, and all the flare decay phase for times when *RHESSI* was making solar observations. Generally, spectra in the A0 state were fitted over the energy range 4.7–10 keV, so avoiding any pulse pile-up peak at  $\sim 15$  keV. *RHESSI* continuum spectra early in the flare rise phase in the A0 attenuator state were often poorly fitted (as shown by the reduced  $\chi^2$ ) with isothermal spectra from the MEKAL code. The agreement became progressively worse for higher count rates until the attenuator state changed to A1.

We attribute this poor agreement to a combination of non-isothermal emitting plasma early in the flare and the degradation of spectral resolution at high count rates, as indicated in §2. Figure 2 illustrates this. Again, for flares in the A1 attenuator state, fits to observed spectra in the rise phase of the flare gave higher  $\chi^2$  than fits during the flare decay, when reduced  $\chi^2 \lesssim 1$  could usually be achieved. A case in point is the M2 flare on 2003 April 26 (Table 1: flare no. 17). For these and most other A1 spectra analyzed, the energy range of the fits were from 5.7 or 6.0 keV to 14 keV or more (see Fig. 3). Note that because of the strong attenuation below  $\sim 6$  keV and the K-escape events mentioned above, no information can be obtained about the incident photon spectrum at lower energies. Many of the results given here are for flares in their decay stage when *RHESSI* was in the A1 state.

In the A3 attenuator state, there was often a poor fit. A significant reason for this is the appearance of an instrumental line feature at about 10 keV, so a total of three lines with Gaussian shapes must be included in the fit (see Fig. 4). The origin of the  $\sim 10$ -keV line feature is under investigation. It may be due to incorrectly subtracted radioactive decay line radiation from the Ge detectors or possibly  $L\beta$  line emission from the tungsten collimators above detectors 2–9. Part of the line feature at  $\sim 8$  keV that we have attributed to the Fe/Ni line feature may be the tungsten  $L\alpha$  line at 8.4 keV.

Another factor possibly contributing to the poor fits obtained in the A3 state is that flares are often near their maximum at those times. It is likely that the emitting plasma departs from being isothermal, causing our isothermal model to give poor fits. The energy range of the fits to A3 spectra was generally 5.7 or 6.0 keV to as high as 30 keV.

Element abundances (particularly the iron abundance) affect intensities of both the observed line features and the free-bound emission. As indicated above, the MEKAL code with cosmic abundances (Allen 1973) was used in OSPEX for all of our analysis. Cosmic element abundances relative to H are very similar to solar photospheric abundances, differing by  $< 0.25$  in the logarithm. There are several indications that, in general, flare plasmas have coronal abundances (Fludra & Schmelz 1995; Phillips 2004; Sylwester et al. 2005b), for which the coronal abundances of elements with first ionization potentials  $< 10$  eV (including Fe and Ni) are enhanced over their photospheric values by a factor of  $\sim 4$  (Feldman & Laming 2000). Eventually, Version 5.1 of the CHIANTI atomic database and code will be used in the analysis software (Landi et al. 2005) with the option of using coronal abundances. Meanwhile, we note that comparison of the continua in the 2–12 keV energy range shows that the MEKAL continua calculated for cosmic abundances are a factor of  $\sim 2$  less than the CHIANTI continua calculated for coronal abundances. The energy dependence is the same in the two cases. Values of  $T_e$  from our analysis are therefore likely to be the same regardless of the spectral code, but our emission measures are likely to be a factor of  $\sim 2$  less than those from analyses

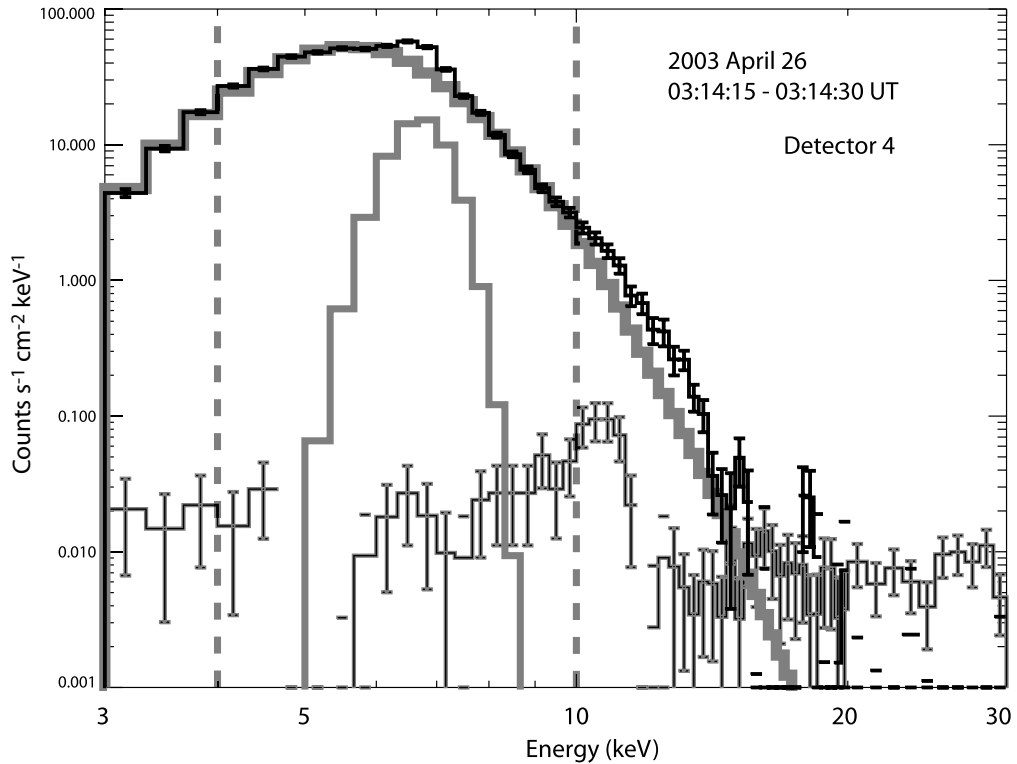


Fig. 2.— Count rate spectra ( $\text{counts s}^{-1} \text{cm}^{-2} \text{keV}^{-1}$ ) in the energy range 3–30 keV from *RHESSI* detector 4 in the A0 attenuator state. The spectrum is during the flare on 2003 April 26 (03:14:15–03:14:30 UT). The histogram with thin dark line and error bars show the observed count rate spectrum with uncertainties in each energy bin. The background spectrum is the histogram with error bars at a count rate level of  $\sim 0.01$ . The histograms with thick gray lines show the MEKAL continuum folded through the spectral response matrix and the line feature with Gaussian shape representing the Fe-line (energy  $\sim 6.7$  keV). The fit range was 5–10 keV (indicated by vertical dashed lines).

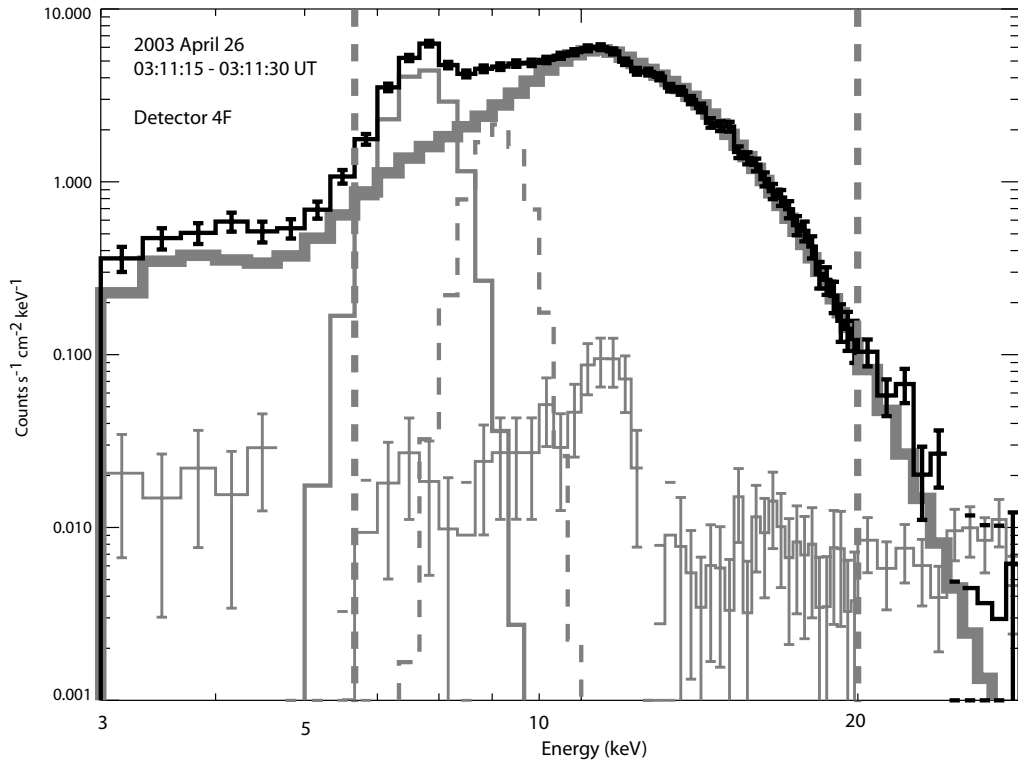


Fig. 3.— As for Fig. 2 but for *RHESSI* detector 4 in the A1 attenuator state during the 2003 April 26 flare (03:11:15–03:11:30 UT). A second line feature with peak energy  $\sim 8$  keV (dashed gray histogram) represents the Fe/Ni line. The fit range indicated by vertical gray lines was 5.7–20 keV.

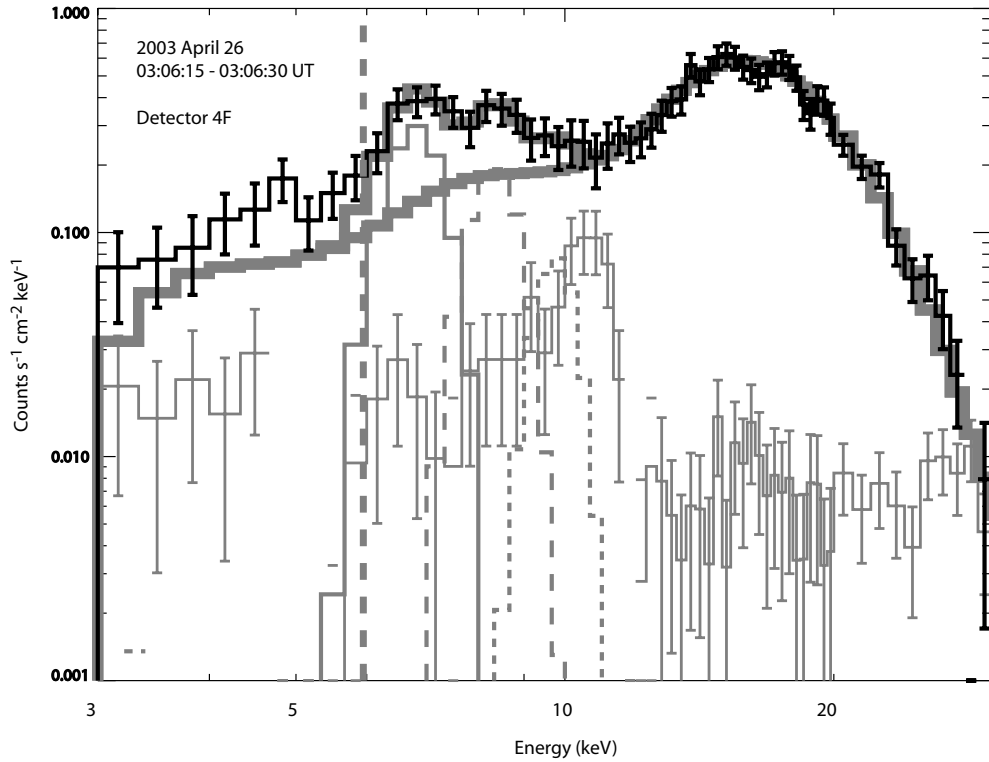


Fig. 4.— As for Fig. 2 but for *RHESSI* detector 4 in the A3 attenuator state during the 2003 April 26 flare (03:06:15–03:06:30 UT). The Fe and Fe/Ni line features are indicated as in Fig. 3. A third line feature has been added (gray histogram with short dashes) in an attempt to fit an instrumentally formed line at  $\sim 10$  keV. The fit range was 6–30 keV.

using CHIANTI with coronal abundances.

*RHESSI* photon spectra have been compared with those derived from the RESIK crystal spectrometer (Sylwester et al. 2005a) on *CORONAS-F*, which operated between 2001 and 2003. This indicates that the *RHESSI* absolute fluxes at energies  $\gtrsim 5$  keV are accurate to  $\sim 20\%$ . RESIK is believed to be calibrated in absolute sensitivity to better than 20% in its first-order mode (energy range of 2.0–3.7 keV) with an energy resolution of  $\lesssim 8$  eV or better. Although there is no overlap with the *RHESSI* energy range, the agreement of the extrapolated spectra is to within the estimated uncertainties of the flux calibration of both instruments for a period during the 2003 April 26 when *RHESSI* was in its A0 state (Dennis et al. 2005). This has been found for several other flares also, with *RHESSI* in A0. On the occasions when RESIK operated in its third diffraction order, the 6.7-keV Fe-line feature is included in one of its four channels; the agreement between RESIK and *RHESSI* estimates of the total flux in this line feature is estimated to be  $\lesssim 50\%$  for flux measurements during the 2003 April 26 flare.

#### 4. Results and Discussion

Table 1 gives details of the 30 flares between 2002 and 2005 analyzed in this work. The serial numbers given in Col. 1 are those referred to in §3. The *GOES* X-ray importance of these flares ranges from C2 to X8. The times of *RHESSI* spectral analysis and the attenuator states are given.

Figure 5 shows the *RHESSI* count rates in three energy bands (background-subtracted), as well as the time histories of estimated values of emission measure,  $T_e$ , and the flux and equivalent width of the Fe-line feature during the M2 flare of 2002 May 31 (No. 6 in Table 1). Over this interval as well as the flare peak, *RHESSI* was in the A1 state. No significant non-thermal component is apparent, a short impulsive phase having occurred at about 23:57 U.T. on May 30, as indicated by counts in the 16–22 keV range. A fit to 68 spectra over the range 5.3–16.7 keV in 20-s intervals shows close agreement between observed spectra and model spectra having the MEKAL continua and two line features to match the Fe and Fe/Ni line features, with reduced  $\chi^2$  steadily decreasing from approximately 1.2 at the earlier times to 0.8 at later times. The Fe-line feature remains strong, with estimated centroid position at  $\sim 6.7$  keV. An isothermal emitting plasma appears to be a good approximation for all spectra over the decline of this flare.

The estimated equivalent widths of the Fe-line feature were plotted against  $T_e$  for all intervals and compared with the theoretical values, taken from a revised version of that given

Table 1. Analyzed *RHESSI* flares

Year	Date	Approx. GOES U.T. range Start-Peak-End <sup>a</sup>	GOES class*	Heliographic coordinates*	Approx. UT range of analyzed <i>RHESSI</i> data	RHESSI attenuator state(s) in the analyzed UT range	
1	2002	Mar. 10/11	10/22:21 - 10/23:25 - 11/00:29	M2.3	S08 E58	10/22:57 - 11/01:13	A1
2		Mar. 15/16	15/22:09 - 15/23:10 - 16/00:42	M2.2	S08 W03	15/23:33 - 16/00:30	A1
3		Apr. 14/15	14/23:34 - 15/00:14 - 15/00:25	M3.7	N19 W60	14/23:51 - 15/00:51	A1
4		Apr. 21	00:43 - 01:51 - 02:38	X1.7	S14 W84	02:09 - 06:20	A1 - A0
5		May. 07	08:46 - 08:52 - 08:55	C2.8	S20 W18	08:52 - 08:57	A0
6		May. 31	00:04 - 00:16 - 00:25	M2.4	N12 W48	00:08 - 00:30	A1
7		Jun. 01	03:50 - 03:57 - 04:01	M1.6	S19 E29	03:53 - 04:03	A1
8		Jul. 20/21	20/21:04 - 20/21:30 - 20/21:54	X3.3	N17 E72	20/22:29 - 21/00:38	A1
9		Jul. 23	00:18 - 00:35 - 00:47	X4.8	S13 E72	01:00 - 02:30	A1
10		Jul. 26/27	26/22:36 - 26/22:38 - 26/22:41	M4.6	S19 E26	26/23:01 - 27/00:01	A1
11		Jul. 29	10:27 - 10:44 - 11:13	M4.7	S11 W15	10:50 - 11:26	A1
12		Aug. 24	00:49 - 01:12 - 01:31	X3.1	S02 W81	01:34 - 02:34	A1
13		Oct. 04	05:34 - 05:38 - 05:41	M4.0	S18 W08	05:41 - 05:48	A1
14		Dec. 02	19:19 - 19:27 - 19:33	C9.6	N09 E32	19:26 - 19:32	A1
15		Dec. 17	22:57 - 23:35 - 23:45	M1.6	S27 E01	23:20 - 23:52	A0 - A1
16	2003	Apr. 23	00:57 - 01:06 - 01:30	M5.2	N18 W16	01:02 - 01:17	A1
17		Apr. 26	03:01 - 03:06 - 03:66	M2.1	N19 W66	03:04 - 03:29	A3 - A1 - A0
18		May. 29	00:51 - 01:05 - 01:12	X1.1	S07 W31	00:45 - 01:21	A0 - A1
19		Aug. 14	22:28 - 22:44 - 23:15	C5.0	S17 W87	22:40 - 22:52	A1 - A0
20		Aug. 19	09:45 - 10:06 - 10:25	M2.7	S15 W68	09:59 - 10:45	A1
21		Oct. 22	19:47 - 20:07 - 20:28	M9.9	S17 E88	20:16 - 20:37	A1
22		Oct. 23	19:50 - 20:04 - 20:14	X1.1	S17 E88	19:59 - 20:31	A3 - A1
23		Nov. 02	17:03 - 17:25 - 17:39	X8.3	S18 W59	18:37 - 19:36	A1
24		Nov. 11	15:23 - 16:15 - 17:17	C8.5	S00 E90	16:00 - 18:10	A1 - A0
25	2004	Jan. 05	02:50 - 03:45 - 05:20	M6.9	S10 E36	04:06 - 04:52	A1
26		Jul. 20	12:22 - 12:32 - 12:45	M8.7	N10 E33	12:37 - 12:47	A3 - A1
27	2005	Jan. 15/16	15/22:25 - 15/23:02 - 15/23:31	X2.6	N14 W08	16/01:30 - 16/03:13	A1
28		Jan. 17	06:59 - 09:52 - 10:07	X3.8	N14 W67	10:07 - 10:38	A1
29		Jan. 20	06:36 - 07:00 - 07:26	X7.9	N14 W67	07:55 - 08:38	A1
30		May. 13	16:13 - 16:57 - 17:28	M8.0	N11 E11	19:49 - 23:47	A0

<sup>a</sup>Data from NOAA *Solar X-ray Flares* and the Lockheed Martin Solar and Astrophysics Laboratory *Latest Events Archive*

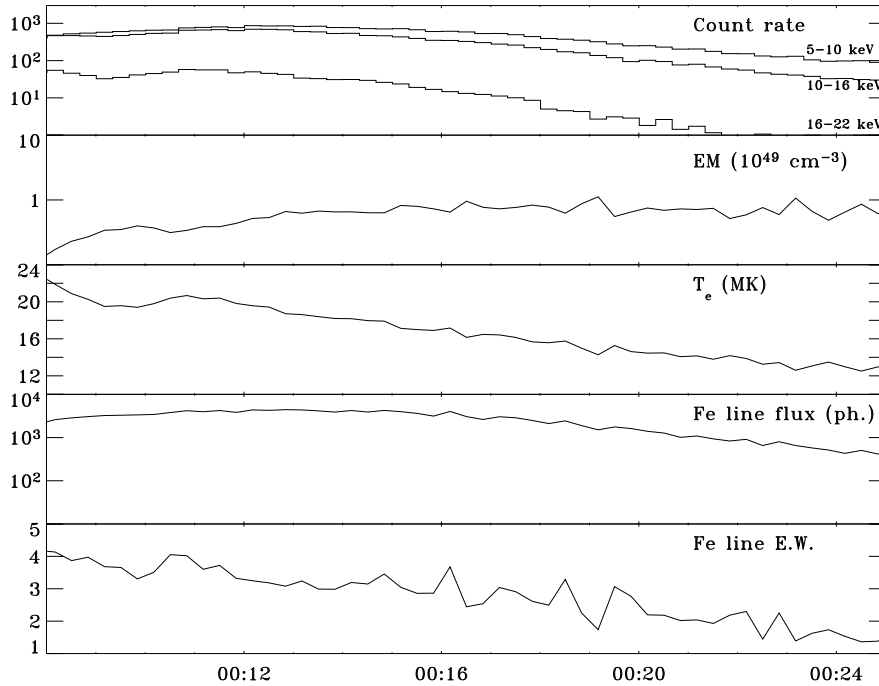


Fig. 5.— *RHESSI* 5-10 keV, 10-16 keV and 16-22 keV count rates ( $\text{s}^{-1}$ ), emission measure (EM, units of  $10^{49} \text{ cm}^{-3}$ ) and  $T_e$  (MK) (both derived from the continuum), Fe-line feature flux (‘ph.’ = photons  $\text{cm}^{-2} \text{ s}^{-1}$ ) and equivalent width (keV) for the M2 flare on 2002 May 31 (No. 6 in Table 1). The peak of the flare in *GOES* was at 00:16 U.T. The background spectrum in a 40-s night time interval before the flare, at approximately 23:55 U.T., was subtracted from the measured count rate spectrum in each time interval during the flare. The uncertainties in these plots are indicated by the scatter of points about smooth curves through the points in each case.

by Phillips (2004). (The theoretical curve has been revised as a result of a changed definition of the continuum flux at the line energy. The maximum of the revised theoretical equivalent width is now 4 keV at  $T_e \sim 24$  MK; the maximum of the previous curve of Phillips (2004) was 3 keV at  $T_e \sim 23$  MK.) Figure 6 (first panel) shows this plot for the 2002 May 31 (No. 6) flare including all points shown in Fig. 5. There is good agreement with the theoretical curve (the maximum observed equivalent width is  $4.2 \pm 0.2$  keV) apart from the fact that the observed points are displaced by a constant temperature difference of about 2 MK, and

Other equivalent width plots show varying degrees of agreement with the theoretical curve. Four broad categories of the degree of agreement between the observed and theoretical equivalent widths can be recognized in the plots. Three flares showing good agreement (type ‘A’) include the flare of 2002 May 31; the observed equivalent widths and theoretical curves are shown in the three panels of Figure 6, with numbers indicating the flare number in Table 1. Some seven flares belong to a category for which the observed equivalent widths increase with  $T_e$  to values above the theoretical curve; the equivalent width plots for these flares are shown in Figure 7 (type ‘B’). Four flares with observed equivalent widths mostly falling below the theoretical curve are shown in Figure 8 (type ‘C’). Many of the points with high values of equivalent widths are from A3 spectra in this category. Finally, eight flares have equivalent widths that rise with  $T_e$  to values roughly as predicted by the theoretical curve, but with the observed points displaced from the curve by a temperature difference of about 1 to 3 MK: see Figure 9 (type ‘D’). Some at least are not very distinguishable from type ‘A’ plots, but for many the temperature range is too small to be certain. The remaining eight flares not shown in Figs. 6, 7, 8, and 9 have too few points with acceptable reduced  $\chi^2$  to categorize.

In summary, equivalent widths of the Fe-line feature, when plotted against  $T_e$ , are close to the theoretical curve for spectra in the A1 attenuator state in the decline of most flares, though with observed equivalent widths lower than predicted by an amount that is a function of energy. The theoretical curve assumes a coronal value for the relative abundance of Fe ( $\text{Fe}/\text{H} = 1.26 \times 10^{-4}$ ) and ionization fractions of Mazzotta et al. (1998). For some flares, in category ‘C’, the observed equivalent widths fall below the theoretical curve, but for some, in category ‘B’, the observed points are higher than the theoretical curve for high values of  $T_e$ . The two well observed flares of 2002 May 31 and 2003 August 19 (Nos. 6 and 17 in Table 1), for which spectral fits having reduced  $\chi^2$  consistently less than about 1.0 were obtained, have equivalent widths very near to the theoretical curve, but with a tendency for the observed points to lie on the higher-temperature side of the theoretical curve (category ‘A’; Fig. 6). Equivalent widths derived when *RHESSI* was in the A1 state on the flare rise phase do not generally agree as well with the theoretical curve, and often have poorer fits as measured by reduced  $\chi^2$ . Equivalent widths in the A0 state are small for low temperatures,

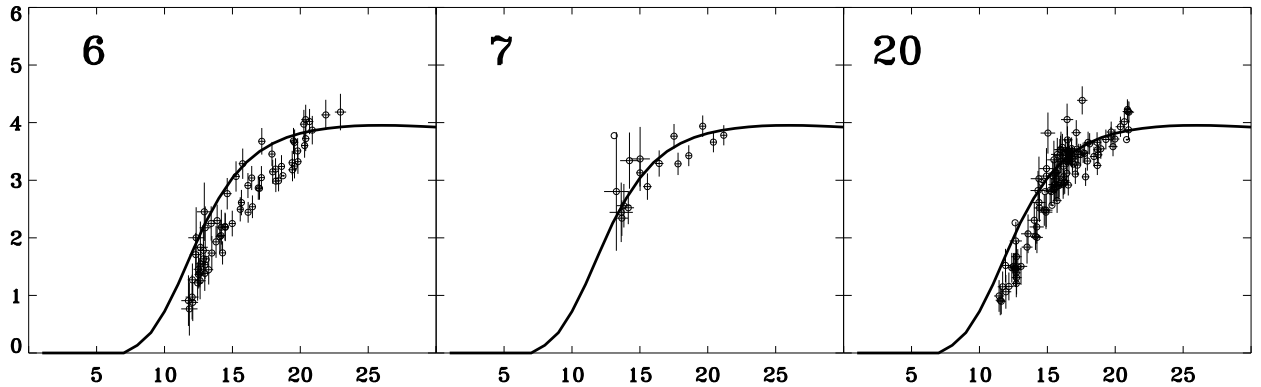


Fig. 6.— Measured values of the Fe-line feature equivalent width (keV, vertical axis) against  $T_e$  (MK, horizontal axis) for three flares in Table 1 (numbers are serial numbers from Col. 1 of table). The curve is the theoretical equivalent width vs.  $T_e$  for a coronal abundance of Fe ( $\text{Fe}/\text{H} = 1.26 \times 10^{-4}$ ). These flares are in the ‘A’ category (good agreement of observed equivalent widths with theoretical curve).

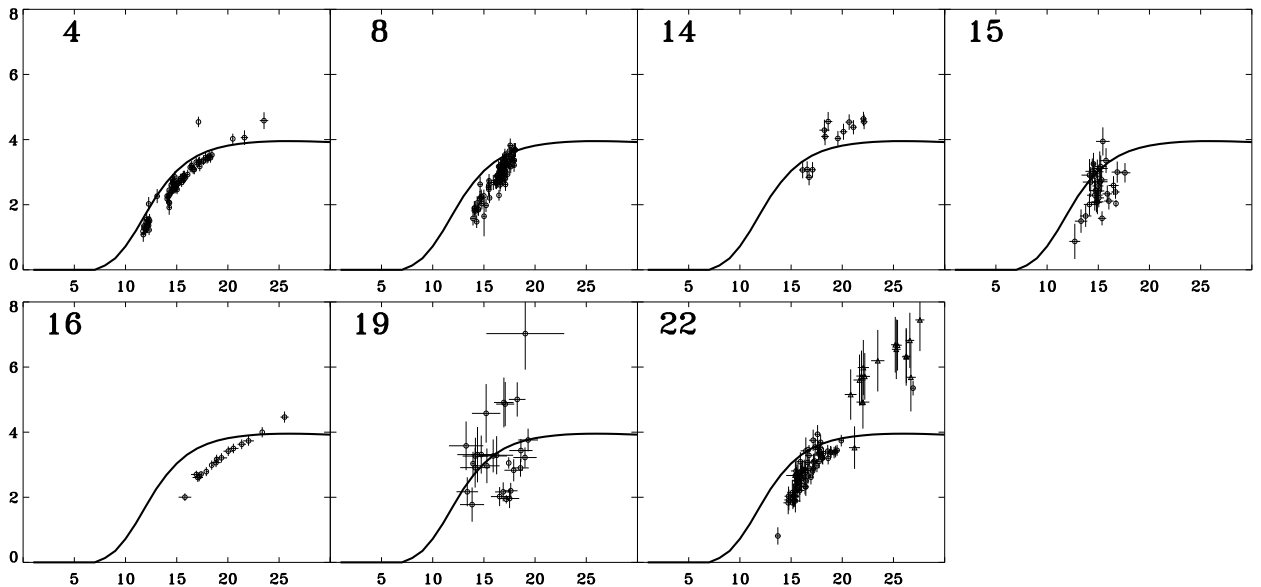


Fig. 7.— As for Fig. 6 but for seven flares in the ‘B’ category (observed equivalent widths increasing with  $T_e$ , with values at high  $T_e$  higher than the theoretical curve. Most points are from the A1 attenuator state, but some A3 points (generally those at higher  $T_e$  with larger error bars) are included).

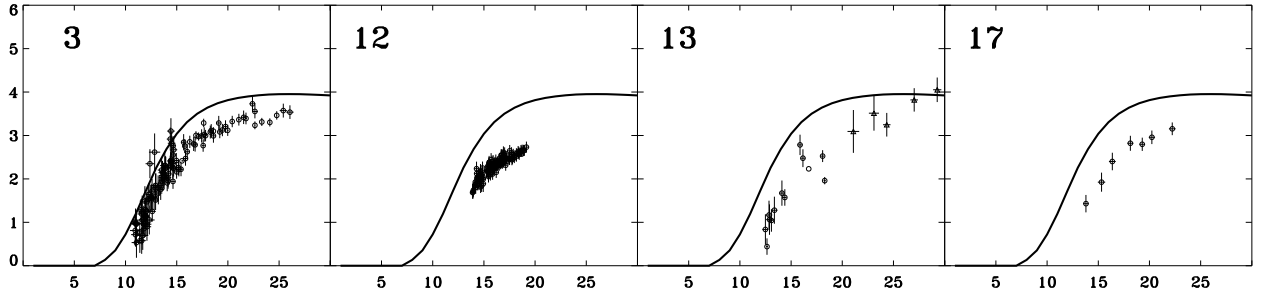


Fig. 8.— As for Fig. 6 but for four flares in the ‘C’ category (observed equivalent widths increasing with  $T_e$  but values always smaller than the theoretical curve). Only A1 points are included.

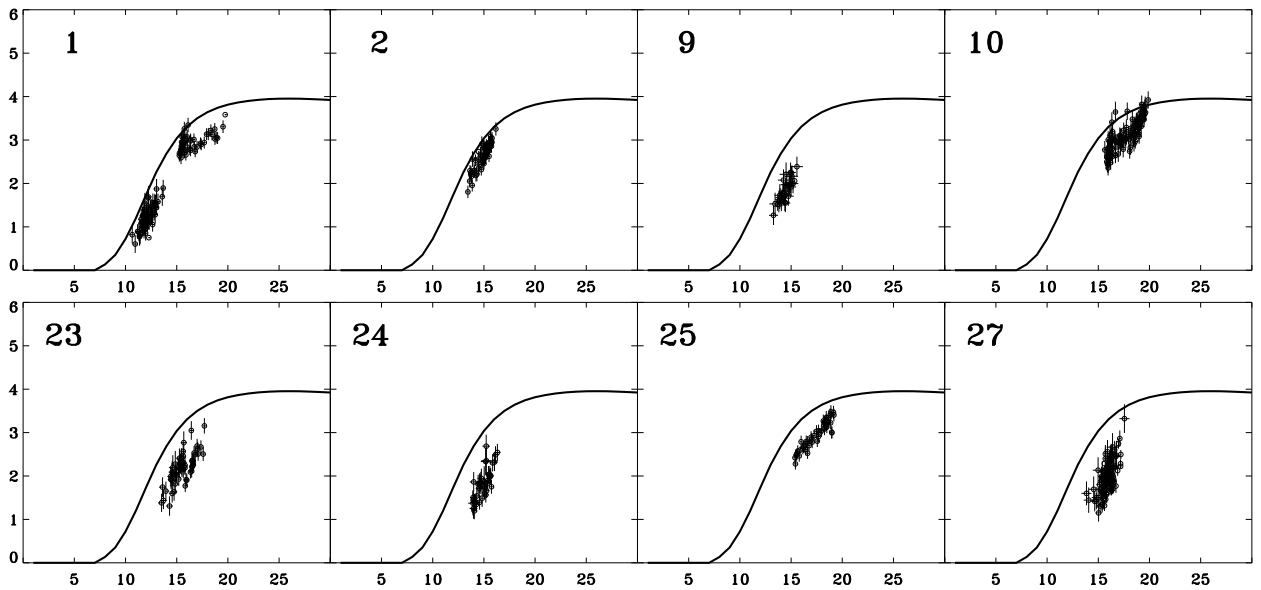


Fig. 9.— As for Fig. 6 but for eight flares in the ‘D’ category (observed equivalent widths increasing with  $T_e$  but with maximum values similar to those indicated by the theoretical curve though with the observed points displaced toward higher temperatures by 2 to 5 MK).

and almost as predicted by the theoretical curve, but for A0 spectra with higher fluxes or temperatures, the agreement with the theoretical curve is poorer. Particularly for A0 spectra near the times of attenuator change to A1 on the rise phase, the Fe-line feature is poorly resolved. Spectra near the maxima of flares in the A3 state are sometimes not well fitted (reduced  $\chi^2 \gtrsim 2$ ), the appearance of the 10 keV instrumental line being an added difficulty in the fit. However, this is not always the case, yet the observed equivalent widths do not often agree well with the theoretical curve.

## 5. Discussion and Conclusions

This analysis of the Fe-line feature in *RHESSI* spectra of 30 solar flares indicates that the line feature's equivalent width is, under certain restricted conditions, close to the theoretical value. The spectra giving the best agreement are those in the *RHESSI* A1 attenuator state during the declining portion of the flare development. These spectra are most often those giving the best fit to model spectra, as measured by the reduced  $\chi^2$ . The analysis assumes an isothermal emitting plasma defined by the electron temperature  $T_e$ . There is a tendency for the observed equivalent widths to lie to the high- $T_e$  side of the theoretical curve which assumes a coronal relative abundance of Fe ( $\text{Fe}/\text{H} = 1.26 \times 10^{-4}$ , or  $4\times$  photospheric) and the ionization fractions of Mazzotta et al. (1998). Some equivalent width plots show the observed points lying below the theoretical curve, by up to 20%, others with observed points lying above the theoretical curve at high  $T_e$  ( $\gtrsim 22$  MK). This may indicate different Fe abundances in different flares.

If the isothermal approximation can be assumed to be correct during the decay phase of these flares, a conclusion from this analysis is that for most flares the coronal relative Fe abundance ( $\text{Fe}/\text{H} = 1.26 \times 10^{-4}$ ) is appropriate for flare plasmas. For some flares ('C' category flares in this sample), the relative Fe abundance may be lower than the coronal value by up to 20%. There is a possibility that the relative Fe abundance is higher than coronal for flares with particularly high temperatures, but there is also a likelihood that the A3 spectra giving these high equivalent widths are not very reliable owing to the difficulty of achieving spectral fits with three lines over a small energy interval (the Fe and Fe/Ni line features and the  $\sim 10$  keV instrumental feature).

The persistent displacement of observed points to the right of the theoretical curve occurs over the temperature range  $12 < T_e$  (MK)  $< 18$ . It could indicate the need for a correction to the ionization fractions of Mazzotta et al. (1998). In particular, the displacement indicates that the value of  $N(\text{Fe}^{+24})/N(\text{Fe})$  (where  $N(\text{Fe}^{+24})$  is the number density of He-like Fe and  $N(\text{Fe})$  the number density of all Fe ions) should be lower than is calculated for the

temperature range  $12 < T_e \text{ (MK)} < 18$ . Antonucci et al. (1987) suggested corrections to the  $N(\text{Fe}^{+23})/N(\text{Fe}^{+24})$  ratio based on *Solar Maximum Mission* crystal spectrometer data. This ratio is equal to  $Q/R$  where  $Q$  is the rate coefficient of ionizations from  $\text{Fe}^{+23}$  and  $R$  the rate coefficient of recombinations to  $\text{Fe}^{+24}$ , both functions of  $T_e$ . Antonucci et al. (1987) argued that, since the various theoretical rate coefficients of ionization from the  $\text{Fe}^{+23}$  available then had more scatter than the rate coefficients of recombinations to  $\text{Fe}^{+24}$ , and that the recombination rates were more slowly varying with  $T_e$  than the ionization rates, the ionization rates were more likely to require revision than the recombination rates downward revision. The ionization rate coefficients in the work of Mazzotta et al. (1998) are based on analytical formulae that are known to be a good representation of measured data for ions up to  $\text{Fe}^{+15}$  (Arnaud & Raymond 1992). However, there is a need for new ionization fractions based on experimental data for ionization rates from  $\text{Fe}^{+23}$  and other ions, now available (e.g. Wong et al. (1993)). Our result is consistent with the number density of  $\text{Fe}^{+24}$  ions being too small compared with that of lower stages like  $\text{Fe}^{+23}$ , but it is difficult to explain why the temperature displacement varies from flare to flare, as we found. It is possible that non-equilibrium effects play a role, but this is unlikely in view of the probable high densities ( $N_e \sim 10^{11} \text{ cm}^{-3}$ ) of the emitting plasma, as was shown by Phillips (2004).

The tendency of Fe-line feature equivalent widths to agree better with theory for periods when flares are in their declining stage and *RHESSI* is in its A1 attenuator state is most likely due to the flares having a more nearly isothermal state in their decay. This has also been found from temperature measurements using Ca XIX and S XV line ratios using the Bragg Crystal Spectrometer on the *Yohkoh* spacecraft (Phillips et al. 2005a). Most likely, flares depart strongly from an isothermal state in their early and peak stages, when images (such as those from *TRACE*, for instance) show some emission in loop top structures at high temperatures co-existing with loop structures with much lower temperatures. The general lack of agreement of Fe line feature equivalent widths observed late in flare developments by *RHESSI* in the A0 state is therefore unexpected on this basis, but this appears to be due, at least occasionally, to the degraded spectral resolution at high count rates and the difficulty of distinguishing the line feature at low count rates and at low temperatures.

Multi-thermal flare plasmas are being investigated and will be the subject of a further analysis of *RHESSI* flare spectra. Differential emission measures,  $\text{DEM} = N_e^2 dV/dT_e$ , can with some difficulty be extracted from spectral line fluxes and other data. Procedures like the PintofAle code (Kashyap & Drake 2000) and DEMON (Sylwester et al. 1980) are currently being compared, using spectral data from *RHESSI*, the *CORONAS-F* RESIK crystal spectrometer, *GOES*, and other broad-band data. Simpler procedures using analytical forms for DEM are also being tried, such as  $\text{DEM} = \exp(T/T_0)$  and  $\text{DEM} = T^{-\alpha}$  (where  $T_0$  and  $\alpha$  are constants for each time interval). It has been found from Si XII dielectronic satellite

line intensity ratios determined from the RESIK instrument that an expression like  $DEM = \exp(T/T_0)$  gives a better agreement with theoretical ratios than an isothermal approximation. The value of  $T_0$  can be simply determined from the ratio of the two *GOES* channels. Again, this is work in progress.

K.J.H.P. acknowledges support from a National Research Council Senior Research Associateship award. C.C.'s work was supported by a Research Assistantship from the Catholic University of America and NASA/GSFC. We are grateful to D. W. Savin, R. A. Schwartz, A. K. Tolbert, and M. Berg for their help.

## REFERENCES

- Allen, C. W., *Astrophysical Quantities*, 3rd Edition, University of London
- Antonucci, E., Dodero, M. A., Gabriel, A. H., Tanaka, K., & Dubau, J. 2005, *A&A*, 1880, 263
- Arnaud, M., & Raymond, J. 2005, *ApJ*, 398, 394
- Caspi, A., et al. 2005, in preparation
- Dennis, B. R., Hudson, H. S., & Krucker, S. 2004, Presented at CESRA Workshop, Isle of Skye
- Dennis, B. R., Phillips, K. J. H., Sylwester, J., Sylwester, B., Schwartz, R. A., Tolbert, A. K. 2005, *Adv. Space Res.*, 35, 1723
- Feldman, U., & Laming, M. 2000, *Phys. Scripta*, 61, 222
- Fludra, A., & Schmelz, J. T. 1995, *ApJ*, 447, 936
- Hurford, G. J., et al. 2002, *Sol. Phys.*, 210, 61
- Kashyap, V. & Drake, J. J. 2000, *BASI*, 28, 475
- Landi, E., et al. 2005, *ApJ*, to be published
- Lin, R. P., et al. 2002, *Sol. Phys.*, 210, 3
- Mazzotta, P., Mazzitelli, G., Colafrancesco, S., & Vittorio, N. 1998, *A&AS*, 133, 403
- Mewe, R., Lemen, J. R., Peres, G., Schrijver, J., & Serio, S. 1985, *A&A*, 152, 229

- Neupert, W. M., White, W. A., Gates, W. J., Swartz, M., & Young, R. M. 1969, *Sol. Phys.*, 6, 183
- Phillips, K. J. H., Sylwester, J., Sylwester, B., & Landi, E. 2003, *ApJ*, 589, L113
- Phillips, K. J. H. 2004, *ApJ*, 605, 921
- Phillips, K. J. H., Feldman, U., & Harra, L. K. 2005, *ApJ*, in press
- Phillips, K. J. H., Dubau, J., Sylwester, J., & Sylwester, B. 2005, *ApJ*, submitted
- Smith, D. M., et al. 2002, *Sol. Phys.*, 210, 33
- Sylwester, J., Schrijver, J., & Mewe, R. 1980, *Sol. Phys.*, 67, 285
- Sylwester, J., et al. 2005, *Sol. Phys.*, 226, 45
- Sylwester, J., Sylwester, B., Phillips, K. J. H., Culhane, J. L., Brown, C., Lang, J., & Stepanov, A. I. 2005, *Adv. Space Res.*, in press
- Wong, K. L., Beiersdorfer, P., Chen, M. H., Marrs, R. E., Reed, K. J., Scofield, J. H., Vogel, D. A., & Zasadzinski, R. 1993, *Phys. Rev. A*, 48(4), 2850